Supporting Information

Non-doped and doped circularly polarized organic light-emitting diodes with high performances based on chiral octahydro-binaphthyl delayed fluorescence luminophores

Zheng-Guang Wu, Zhi-Ping Yan, Xu-Feng Luo, Li Yuan, Wei-Qiu Liang, Yi Wang, You-Xuan Zheng,* Jing-Lin Zuo and Yi Pan

State Key Laboratory of Coordination Chemistry, Collaborative Innovation Center of Advanced Microstructures, Jiangsu Key Laboratory of Advanced Organic Materials, School of Chemistry and Chemical Engineering, Nanjing University, Nanjing, 210023, P. R. China
E-mail: yxzheng@nju.edu.cn

1. General information

1.1 Materials, instruments and measurement

NMR measurements were conducted on a Bruker AM 400 spectrometer. The mass spectra were recorded by Matrix Assisted Laser Desorption Ionization Time of Flight Mass Spectrometry (autoflex TOF/TOF, Bruker Daltonics). High-resolution mass spectra were recorded on a MICROTOF-Q III instrument. Absorption spectra were measured on a UV-3100 spectrophotometer and photoluminescence spectra were obtained from a Hitachi F-4600 photoluminescence spectrophotometer. Cyclic voltammetry measurements were conducted on a MPI-A multifunctional electrochemical and chemiluminescent system (Xi'an Remex Analytical Instrument Ltd. Co., China) at room temperature, with a polished Pt plate as the working electrode, platinum thread as the counter electrode and Ag-$AgNO_3$ (0.1 M) in CH_3CN as the reference electrode, *tetra*-n-butylammonium perchlorate (0.1 M) was used as the supporting electrolyte, using Fc^+/Fc as the internal standard, the scan rate was 0.1 V/s. The absolute photoluminescence quantum yields (Φ) and the decay lifetimes of the compounds was measured with HORIBA FL-3 fluorescence spectrometer. Thermogravimetric analysis (TGA) was performed on a Pyris 1 DSC under nitrogen at a heating rate of 10 ^oC min^{-1}. The circular dichroism (CD) spectra were measured on a JASCO J-810 circular dichroism

spectropolarimeter with 'Standard' sensitivity. The scan speed was set as 200 nm/min with 1 nm resolution and a respond time of 1.0 s. The circularly polarized luminescence (CPPL) spectra were measured on a JASCO CPPL-300 spectrophotometer with 'Standard' sensitivity at 200 nm/min scan speed and respond time of 2.0 s employing "slit" mode.

1.2 Fabrication and measurement of CP-OLEDs

Indium-tin-oxide (ITO) coated glass with a sheet resistance of 10 Ω sq^{-1} was used as the anode substrate. Prior to film deposition, patterned ITO substrates were cleaned with detergent, rinsed in de-ionized water, dried in an oven, and finally treated with oxygen plasma for 5 minutes at a pressure of 10 Pa to enhance the surface work function of ITO anode (from 4.7 to 5.1 eV). All the organic layers were deposited with the rate of 0.1 nm s^{-1} under high vacuum ($\leq 2\times10^{-5}$ Pa). The doped layers were prepared by co-evaporating dopant and host material from two individual sources, and the doping concentrations were modulated by controlling the evaporation rate of dopant. LiF and Al were deposited in another vacuum chamber ($\leq 8.0\times10^{-5}$ Pa) with the rates of 0.01 and 1 nm s^{-1}, respectively, without being exposed to the atmosphere. The thicknesses of these deposited layers and the evaporation rate of individual materials were monitored in vacuum with quartz crystal monitors. A shadow mask was used to define the cathode and to make ten emitting dots (with the active area of 10 mm^2) on each substrate. Device performances were measured by using a programmable Keithley source measurement unit (Keithley 2400 and Keithley 2000) with a silicon photodiode. The EL spectra were measured with a calibrated Hitachi F−7000 fluorescence spectrophotometer. Based on the uncorrected EL fluorescence spectra, the Commission Internationale de l'Eclairage (CIE) coordinates were calculated using the test program of Spectrascan PR650 spectrophotometer. The EQE of EL devices were calculated based on the photo energy measured by the photodiode, the EL spectrum, and the current pass through the device. The circularly polarized electroluminescence (CPEL) spectra were measured on a JASCO CPPL-300 spectrophotometer with 'Standard' sensitivity at 200 nm/min scan speed and respond time of 2.0 s employing "band" mode.

2. NMR Spectra

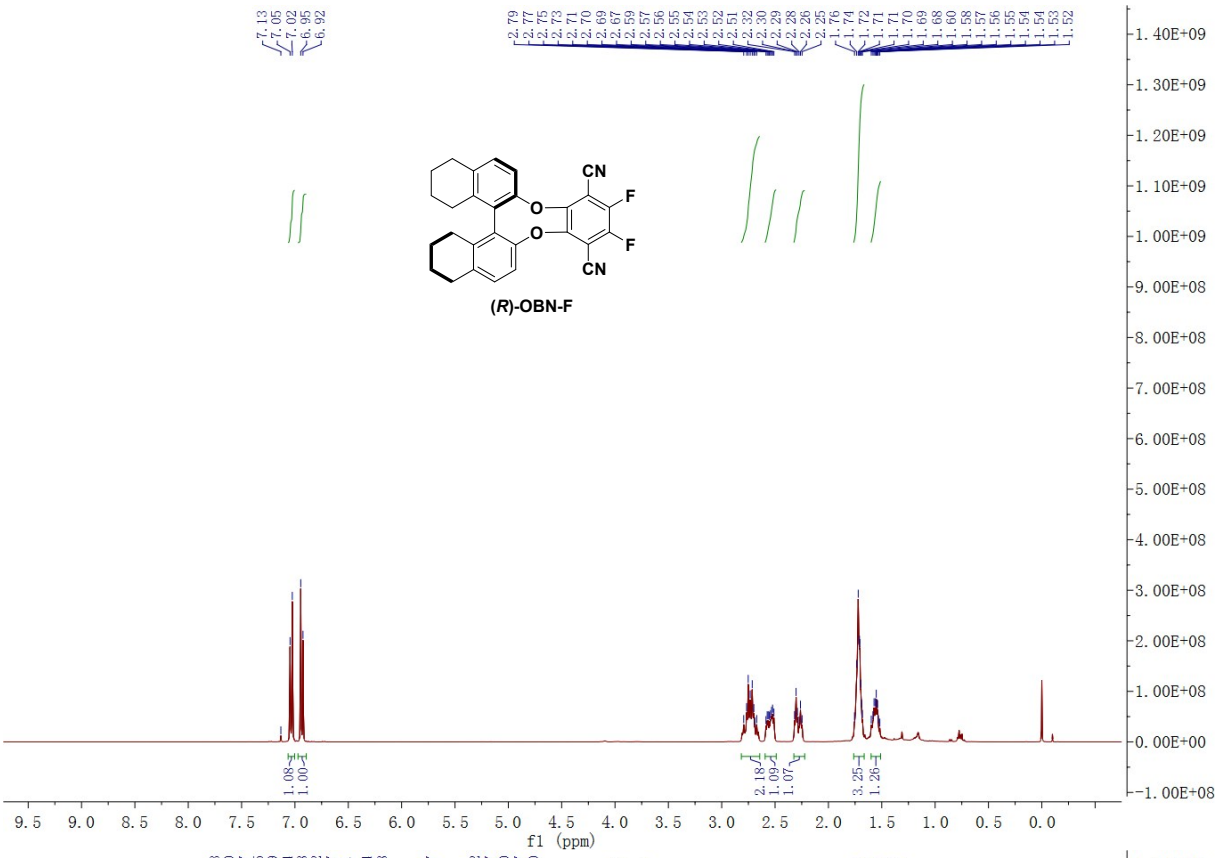

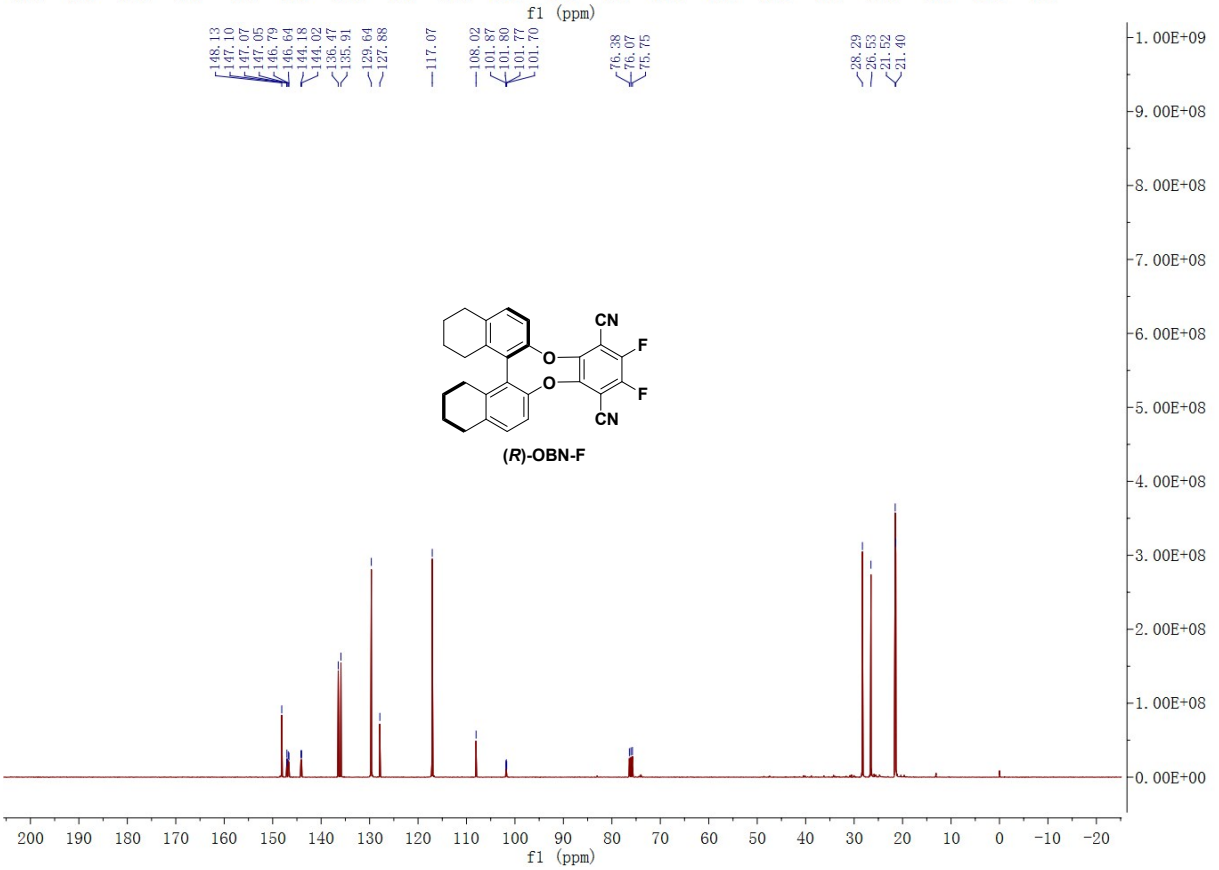

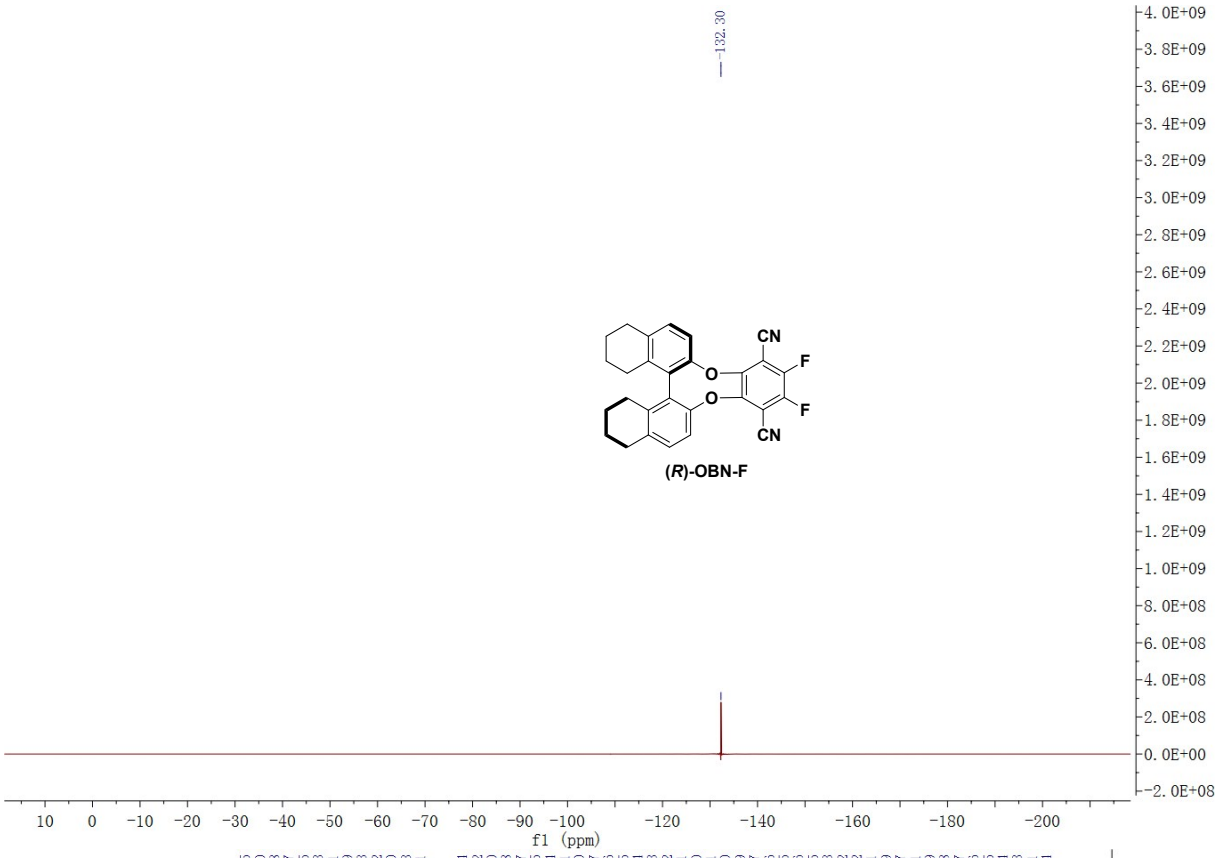
-132.30
CN
F
O
O
F
CN
(R)-OBN-F
f1 (ppm)

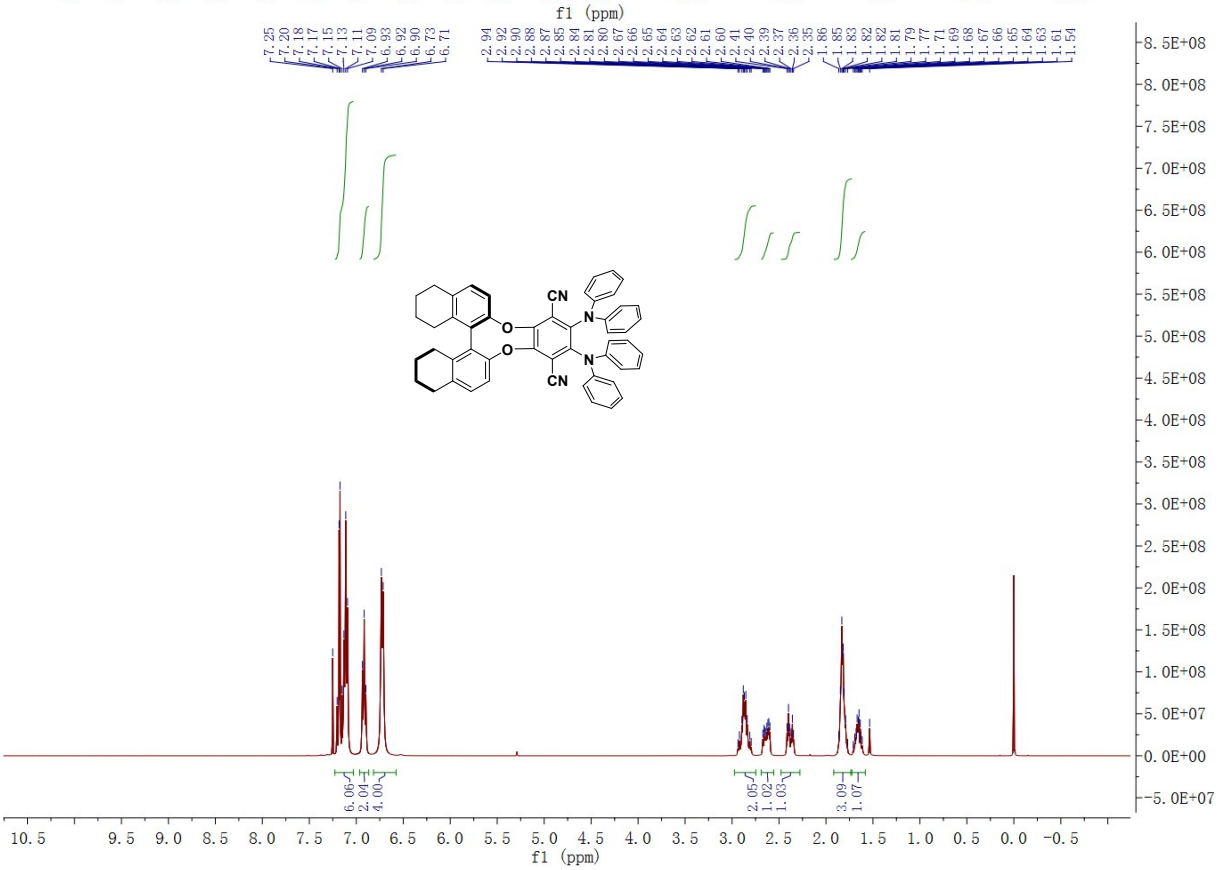
CN
N
O
O
N
CN
6.06
2.04
4.00
2.05
1.02
1.03
3.09
1.07
f1 (ppm)

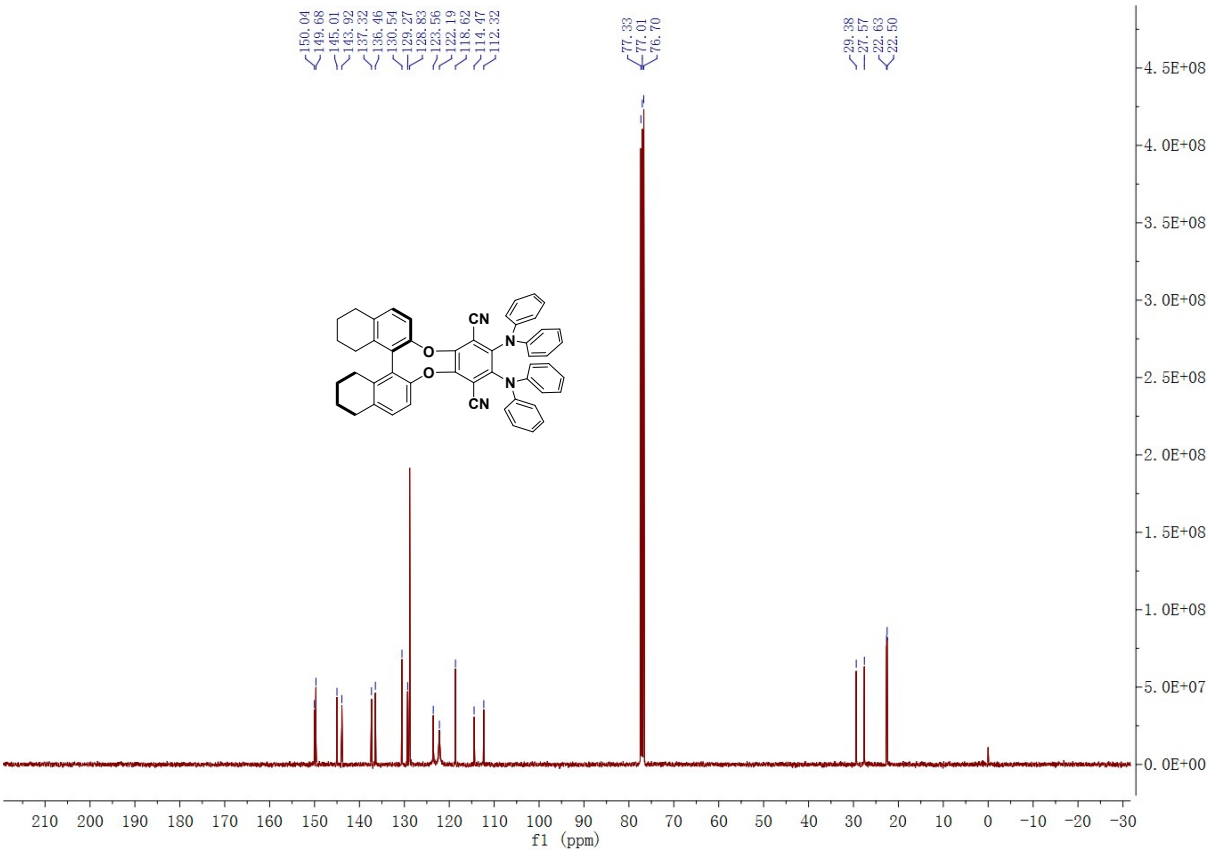

3. Supplementary data

Table S1. The devices performances of all reported CP-OLEDs *vs* this work by **(*R*/*S*)-OBN-DPA**.

Materials	Structures	Device models	λ_{em} [nm]	$\lvert g_{EL} \rvert$	$\eta_{c,max}$ [cd A^{-1}]	EQE %	Luminance [cd m^{-2}]	Ref.
BMB-PPV-*co*-BDMO-PPV	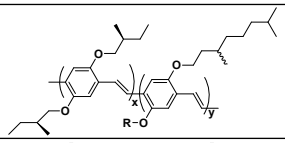	Pure polymer layer	600	1.70×10^{-3}	-	-	-	*J. Am. Chem. Soc*, **1997**, *119*, 9909.
(S)-PF4/1	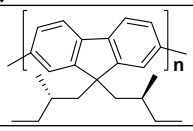	Pure polymer layer	425±5	0.16	-	-	-	*Macromolecules*, **2002**, *35*, 6792. *Adv. Mater*, **2000**, *12*, 362.
(S)-PF4/1-co-PF8	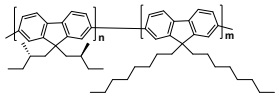			0.05	-	-		
(S)-PF8/1/1	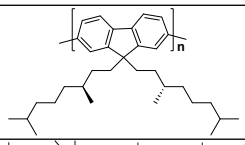			0.25	-	-		
Nonafluorenes Oligomers	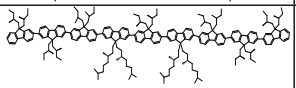	Pure polymer layer	425, 450	0.35	0.94	-	-	*J. Am. Chem. Soc*, **2003**, *125*, 14032.

c-PFBT	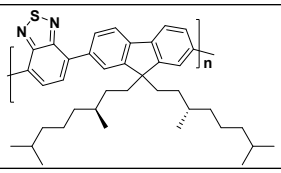	Pure polymer layer	510	0.80	0.12 lm W^{-1}		**80**	*ACS Nano*, **2017**, *11*, 12713.
F8BT	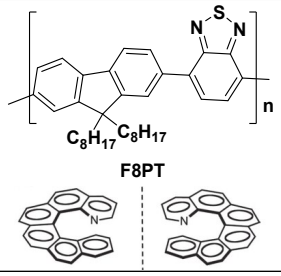	F8BT with chiral semiconducting dopant	540	0.2	1.1 lm W^{-1}	-	**3000**	*Adv. Mater*, **2013**, *25*, 2624.
Chiral Europium Complex	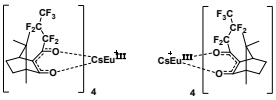	Dispersed in PVK and OXD7	595, 612	0.03-1.41	0.005	**0.0042**	**3**	*Adv. Mater*, **2015**, *27*, 1791. *Adv. Funct. Mater,* **2017**, *27*, 1603719.
Platinahelicene	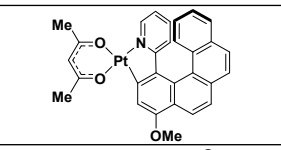	Dispersed in PVK and OXD7	625	0.38	0.52	-	**230**	*J. Am. Chem. Soc*, **2016,** *138*, 9743.
F8BT	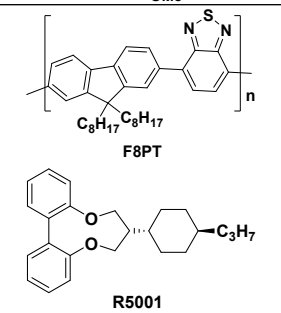	F8BT with chiral R5011	546	1.13	4.46	-	**4000**	*Adv. Mater*, **2017**, *29*, 1700907.
Chiral Iridium Complexes	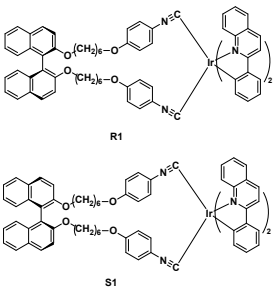	Dispersed in PVK and OXD7	526, 558	10^{-3}	7.5		**4473**	*Adv. Optical Mater*, **2017**, *5*, 1700359
Chiral Iridium Complexes	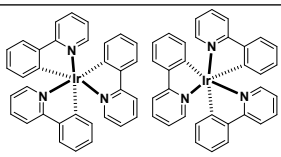	Dispersed in mCP	495-533	$0.28\sim2.6\times10^{-3}$	-	-	-	*Sci. Rep*, **2015**, *5*, 14912.
Chiral AIEgens	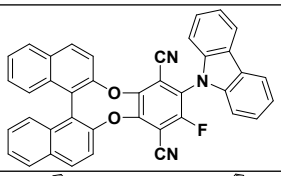	Dispersed in mCP	496	0.026	24.6	**9.3 (4.4 at 1000 cd m^{-2})**	**2948**	*Adv. Funct. Mater*, **2018**, 1800051.
		Pure AIEgens	537	0.06	10.3	**3.5**	**2570**	
Chiral TADF	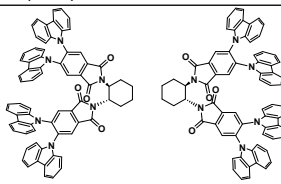	Dispersed in mCBP	520	$1.7\sim2.3\times10^{-3}$	59.4	**19.8 (6.3 at 1000 cd m^{-2})**	**~5000**	*Angew. Chem. Int. Ed*, **2018**, *57*, 1.

AIE-active chiral polymer	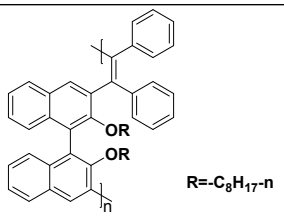	Pure polymer layer	512	0.024	0.926		**1669**	*Chem. Commun*, **2018**, *54*, 9663.
AIE-active chiral polymer	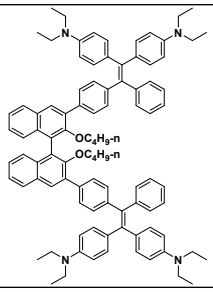	Pure polymer layer	534	3.2×10^{-3}	1.32	**0.48**	**8061**	*Org. Lett*, **2019**, *21*, 439.
CP-TADF molecules	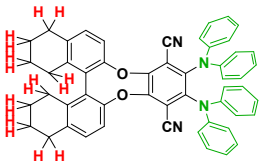 **(*R*/*S*)-OBN-DPA**	**Pure chiral material layer**	**560**	**$2.2\sim2.9\times10^{-3}$**	**23.0**	**6.6 (5.5 at 1000 cd m^{-2})**	**16187**	**This work**
		Dispersed in 26DCzPPy	**543**	**$1.8\sim2.3\times10^{-3}$**	**45.3**	**12.4 (11.5 at 1000 cd m^{-2})**	**25418**	**This work**

Table S2. Crystal data and structure refinement for **(*R*/*S*)-OBN-DPA**.

Identification code	**(*R*)-OBN-DPA**	**(*S*)-OBN-DPA**
CCDC	1896204	1896205
Empirical formula	$C_{52}H_{40}N_4O_2$	$C_{52}H_{40}N_4O_2$
Formula weight	752.92	752.92
Temperature/K	296(2)	296(2)
Crystal system	Monoclinic	Monoclinic
Space group	$P2_1$	$P2_1$
a/Å	9.116(2)	9.1408(7)
b/Å	12.611(3)	12.6631(9)
c/Å	34.215(8)	34.540(2)
α/°	90.00	90.00
β/°	90.00	90.00
γ/°	90.00	90.00
Volume/$Å^3$	3933.4(17)	3998.1(5)

Z	66	45
ρ_{calc}g/cm^3	1.269	1.248
μ/mm^{-1}	0.078	0.077
F(000)	1579.0	1578.0
Radiation	MoKα (λ = 0.71073)	MoKα (λ = 0.71073)
2Θ range for data collection/°	2.38 to 55.52	2.36 to 55.04
Index ranges	$-9 \leq h \leq 11$, $-16 \leq k \leq 15$, $-44 \leq l \leq 43$	$-11 \leq h \leq 11$, $-11 \leq k \leq 16$, $-43 \leq l \leq 44$
Reflections collected	24966	27741
Independent reflections	9157 [R_{int} = 0.1018]	9175 [R_{int} = 0.0866]
Data/restraints/parameters	9157/12/542	9175/384/542
Goodness-of-fit on F^2	1.021	0.980
Final R indexes [I>=2σ (I)]	R1 = 0.0716, wR2 = 0.1527	R1 = 0.0572, wR2 = 0.1216
Final R indexes [all data]	R1 = 0.1232, wR2 = 0.1813	R1 = 0.1405, wR2 = 0.1640
Largest diff. peak/hole / e Å^{-3}	0.33/-0.36	0.26/-0.26
Flack parameter	-1(2)	1.2(19)

$R_1{}^a = \Sigma||F_o| - |F_c||/\Sigma F_o|$. $wR_2{}^b = [\Sigma w(F_o{}^2 - F_c{}^2)^2/\Sigma w(F_o{}^2)]^{1/2}$

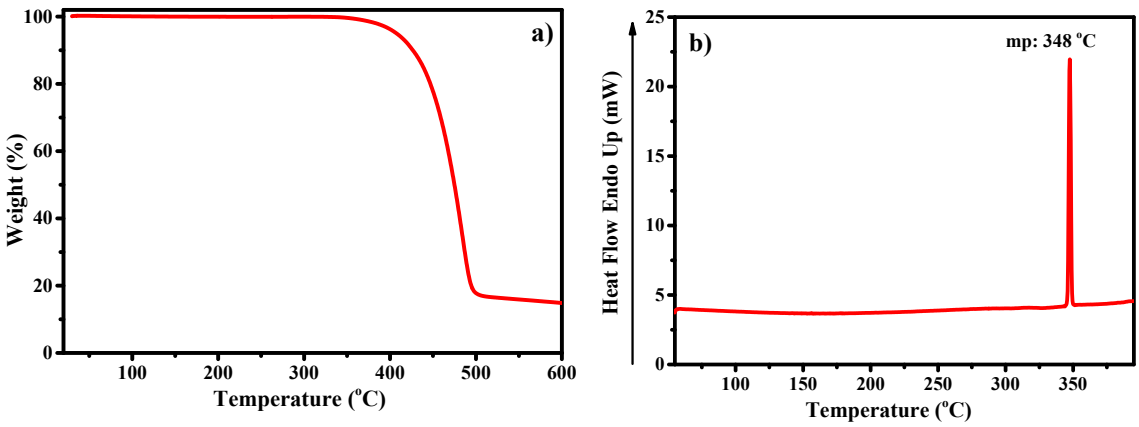

Fig. S1 TGA (a) and DSC (b) curves of **(*R*)-OBN-DPA**.

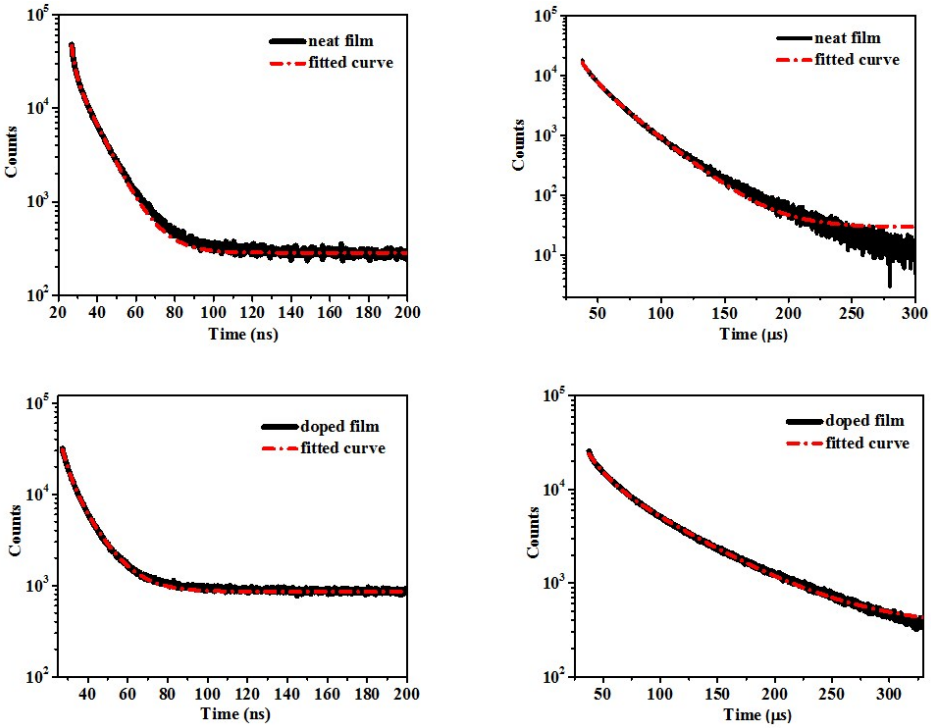

Fig. S2 The transient PL decay curves for prompt and delayed fluorescence lifetimes of **(*R*)-OBN-DPA** in neat and doped film.

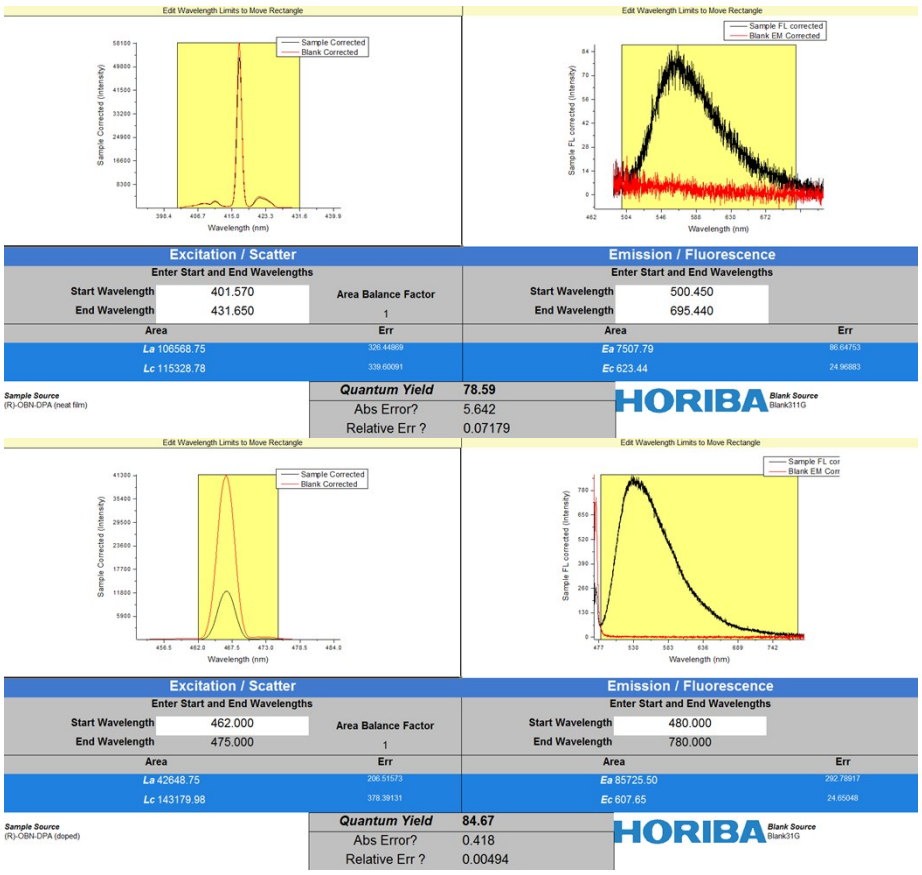

Fig. S3 The photoluminescence quantum yields (PLQYs) of **(*R*)-OBN-DPA** in neat and doped film determined by an integer-sphere system.

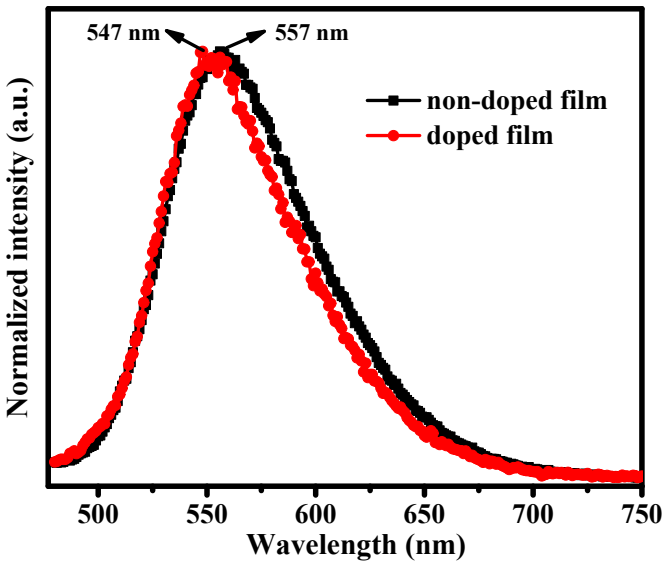

Fig. S4. Fluorescence spectra at room temperature of **(*R*)-OBN-DPA** in non-doped and doped films (10% **(*R*)-OBN-DPA** compound in 26DCzPPy).